

Supplemental Materials

Molecular Biology of the Cell

Nowotarski et al.

Supplemental Figures

Suppl. Fig. 1. Histograms of filopodial lengths and lifetimes, and characterization of filopodial extension and retraction. (A,B) All maximum length histograms bins=0.5 μm intervals. All lifetime histograms bins=100s intervals. (A) Leading edge data using Actin-GFP. (B) Amnioserosa data using Moe ABD-GFP. (C) Seconds to maximum length. (D) Seconds from maximum length to the point when length < 1.15 μm . (E) Ratio of seconds to maximum length/seconds from maximum length. (F) Non-instantaneous rate to maximum length. Statistical tests=ANOVA.

Suppl. Fig. 2. Individual Protrusive profiles for all genotypes. Black line=linear regression fit with corresponding equation. (A) LE vs AS data using Moe ABD-GFP. (B) LE data using Actin-GFP. (C) AS data using Moe ABD-GFP.

Suppl. Fig. 3. Ena-induced tricellular filopodia are polarized. Stage 14 embryos, dorsal up, expressing actin-GFP in *engrailed* stripes. (A) RFP-Ena localizes to tips of ectopic tricellular filopodia (yellow arrows). (B) Ena-induced filopodia at tricellular junctions emerge from the dorsal edge of the cells (yellow arrow) and not from the ventral cell edge (cyan arrow). (C) The protrusive profile of Ena-induced filopodia at tricellular junctions matches that of the few tricellular filopodia we found in embryos only expressing Actin-GFP. Scale bars=10 μm , except A inset = 5 μm .

Suppl. Fig. 4. Overexpressing Ena or active Dia does not substantially affect dorsal closure. (A-C) Movie stills, embryos expressing Moe ABD-GFP driven by the *sqh* promoter in genotypes indicated, filmed from 90 min before closure. Scale bars=50 μm . Dorsal closure is largely unaltered. (D,E) Horizontal line indicates mean and vertical bracket 95% CI. Statistical test = ANOVA. (D) Measuring rate of area change in the last 90 min of closure $\mu\text{m}^2/\text{min}$ revealed no differences. (E) Rate of canthi distance change in the last 90 min of closure. Only Ena overexpression altered this parameter.

Suppl. Fig. 5. *ena* and *dia* zygotic mutants have substantially lower protein levels. Embryos, stage 13-14, dorsal up, with antigens indicated. Scale bars=50 μm . *ena* or *dia* zygotic mutants (identified by loss of a GFP-marked Balancer chromosome) were stained together with wildtype embryos marked with Histone-RFP, to provide a direct comparison of staining levels. (A) *ena*^{GCl}/*ena*⁴⁶ trans-heterozygous

zygotic mutants have substantially reduced Ena levels (insets = closeups of AS). (B) *dia*² zygotic mutants have reduced Dia levels compared to controls.

Suppl. Fig. 6. *dia*² zygotic mutants are embryonic lethal and display potential cell division defects. (A) Embryonic lethality from the indicated crosses, and cuticles of lethal embryos from the cross yielding *dia* zygotic mutants, illustrating phenotypic classes from least to most severe, with corresponding percentage of embryos in each class. Scale bar=25µm. (B) *dia*² zygotic mutants have severe head involution defects (bracket). Scale bars=10µm. (C) Stage 14 *dia*² mutants have larger cells in the lateral epidermis compared to *twi*GFP-marked *dia* heterozygotes. (D) Quantification of number of cells per 400µm². Statistical test=Student's T-test. (E,F) Stage 13 wildtype or *dia*² mutants. Maximum intensity z projection. The LE and lateral epidermal cells of stage 14 *dia*² mutant embryos have many larger cells and nuclei (yellow arrows), though occasional nuclei are normal sized (arrowhead). In contrast, amnioserosal cell nuclei are unaltered from wildtype (magenta arrows), likely due to the fact that AS cells do not divide after the blastoderm stage. Scale bars 20µm.

Supplemental Movies

Suppl. Movie 1. Overview of DC. The last ~3 hours of DC in a control embryo expressing *sqh* Moesin-GFP. Maximum intensity projection of 5µm (0.5µm steps) total every 30s at 40X. Note AS cells extend beneath LE cells, appearing behind the actin cable. All movies play at 20 fps.

Suppl. Movie 2. Comparison of AS and LE protrusions. AS (left) and LE (right) cells at 100x expressing Moe-GFP through *sqh* promoter or UAS-*engrailed*GAL4 respectively.

Suppl. Movie 3. AS filopodia exhibit considerable X-Y lateral motion during lifetime. Two examples of AS filopodia (visualized with Moe-GFP) at 100x with corresponding maximum intensity projections detailing lifetime trajectory.

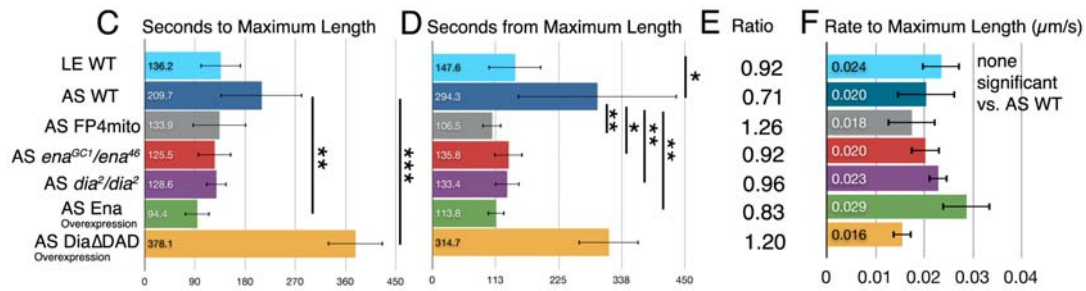
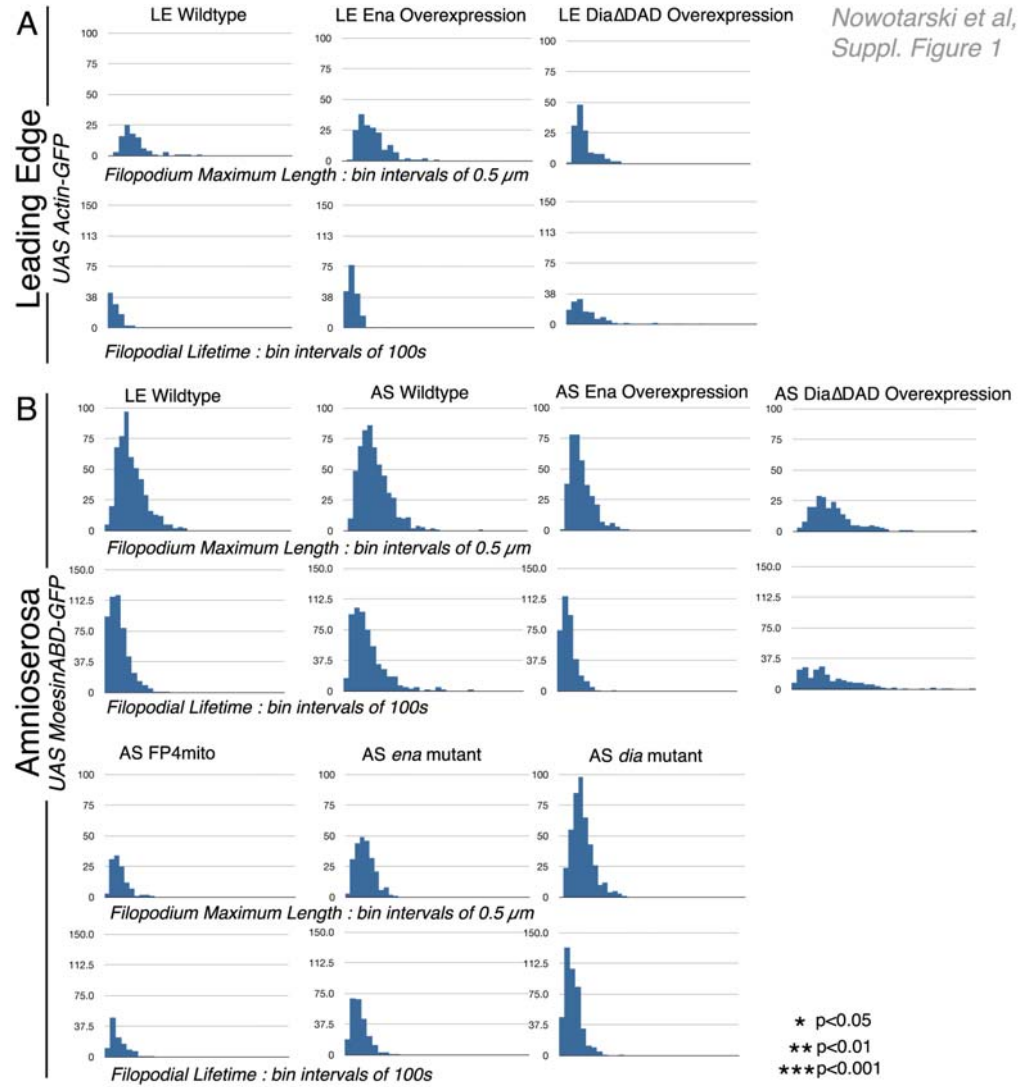
Suppl. Movie 4. Overexpression of Ena and DiaΔDAD at the LE. Wildtype (left), Ena Overexpression (middle) and DiaΔDAD overexpression (right) along the LE. Moe-GFP driven by *engrailed*-GAL4. Images acquired every 5s at 100X.

Suppl. Movie 5. Overexpression of Ena and Dia Δ DAD induce ectopic protrusions in the lateral epidermis at tricellular junctions. Wildtype (left), Ena Overexpression (middle) and Dia Δ DAD overexpression (right) in cells in the lateral epidermis more ventral to the LE. Cyan arrows= dynamic protrusions at tricellular locations in both overexpression conditions while yellow arrow=static lateral protrusions produced only by active Dia. Moe-GFP driven by *engrailed*-GAL4. Images acquired every 5s at 100X.

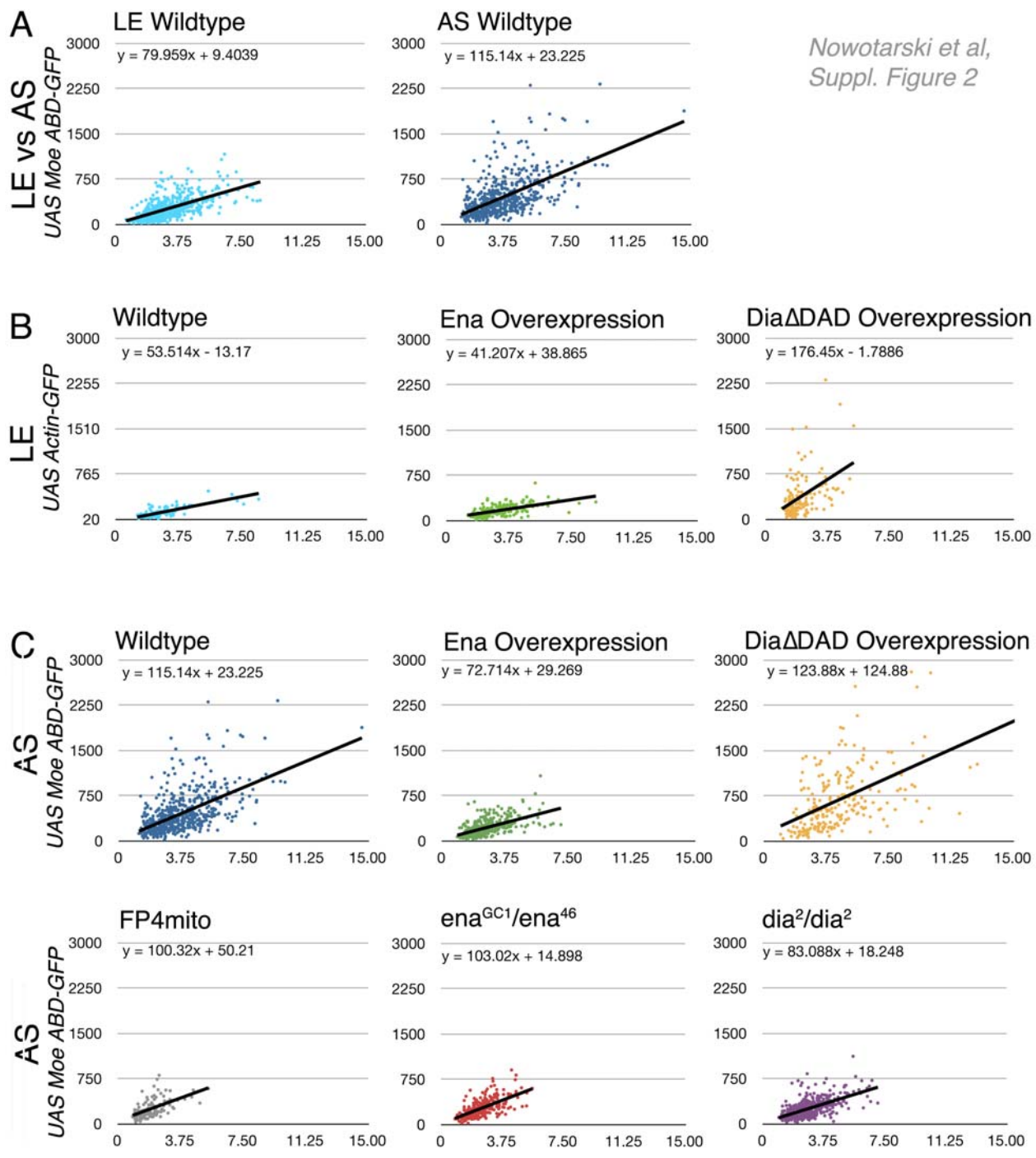
Suppl. Movie 6. Overexpression of Ena and Dia Δ DAD in the AS. Wildtype (left), Ena Overexpression (middle) and Dia Δ DAD overexpression (right) in AS cells. All images are sqh Moe-GFP post bleaching. Images acquired every 5s at 100X.

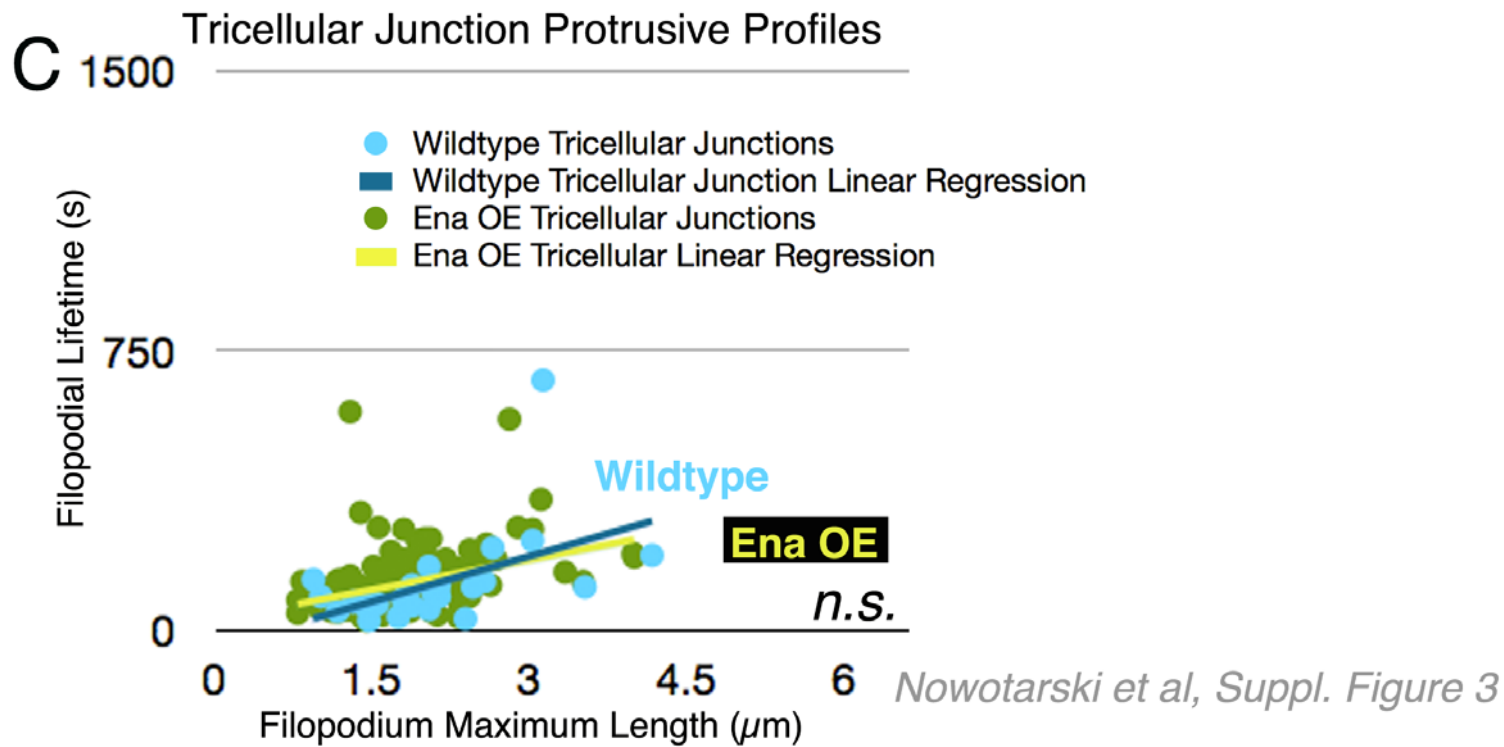
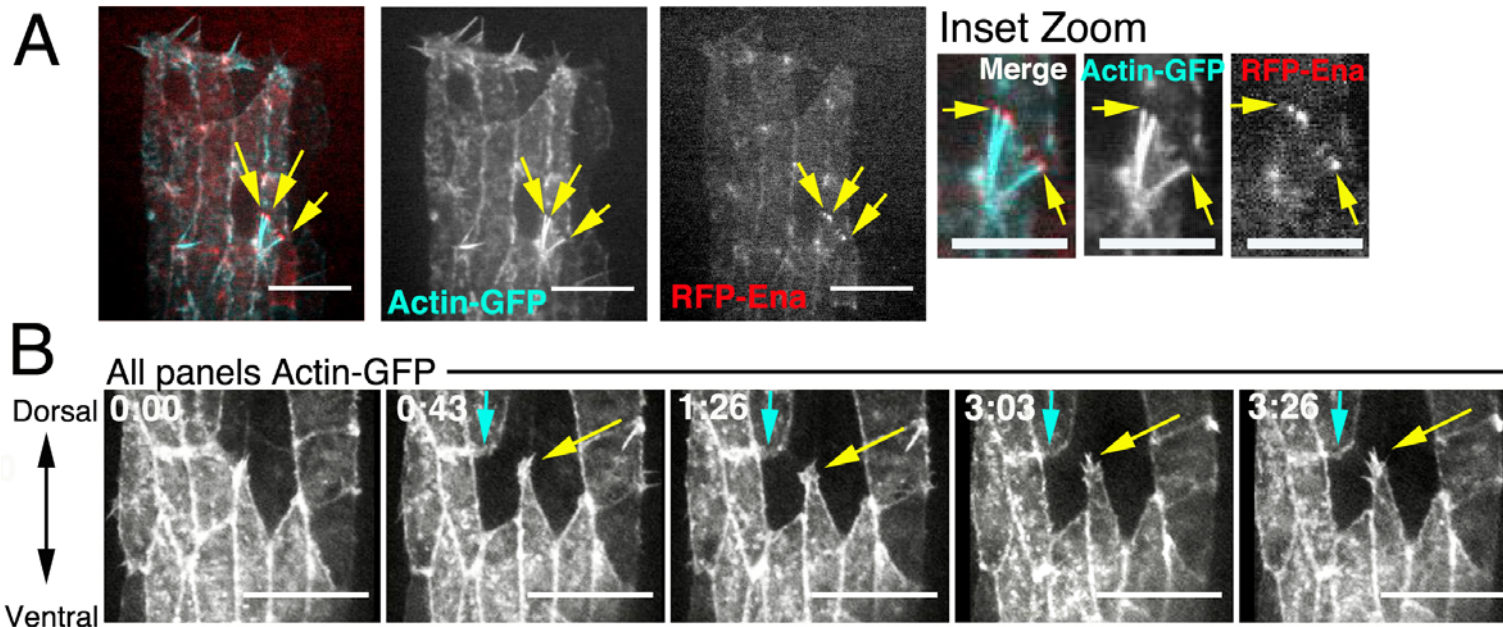
Suppl. Movie 7. Overview of closure in each condition. Left to right: Top row, Wildtype, Ena overexpression in the AS, Dia Δ DAD overexpression in the AS, Bottom row, FP4mito overexpression in the AS, *ena*^{GC1}/*ena*⁴⁶ zygotic mutant, *dia*²/*dia*² zygotic mutant. All images are sqh Moe-GFP 40x, single plane acquired every 15s.

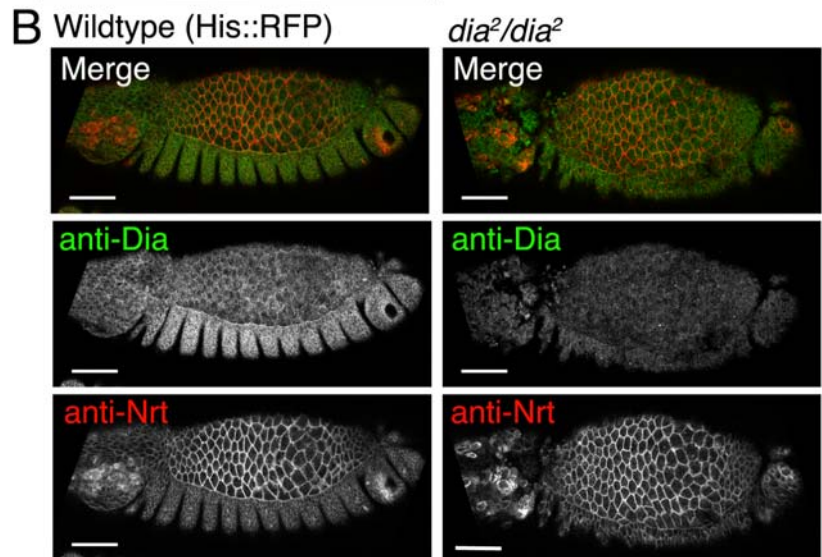
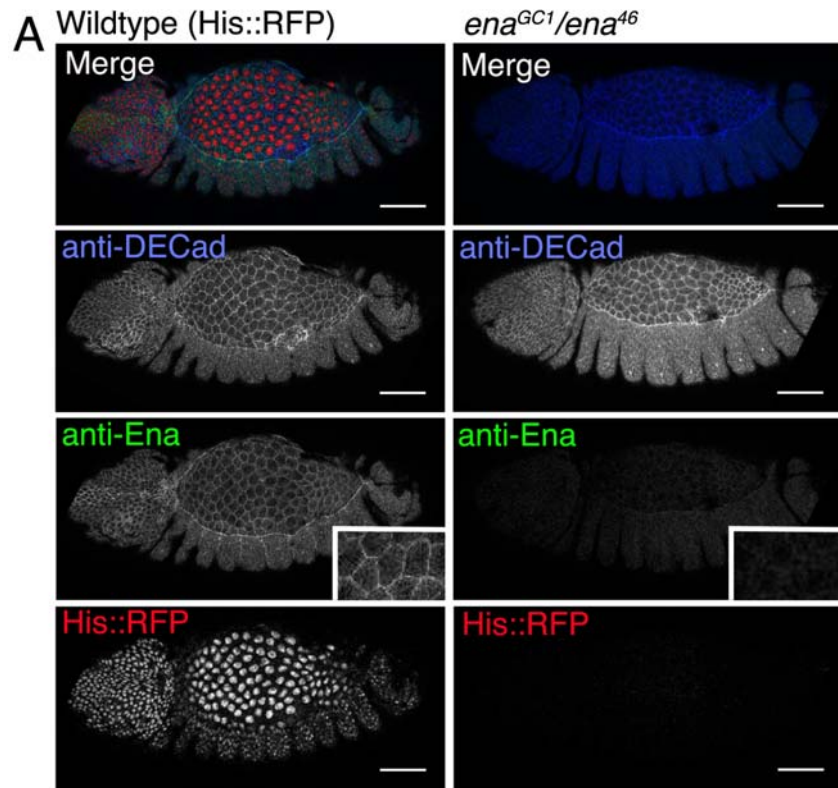
Suppl. Movie 8. The AS upon *ena* and *dia* loss. Left to right: Wildtype, FP4mito expressed using c381 GAL4, *ena*^{46/GC1} zygotic mutant and *dia*²/*dia*² zygotic mutant. All images are sqh Moe-GFP post bleaching. Images acquired every 5s at 100X.



Nowotarski et al,
Suppl. Figure 2







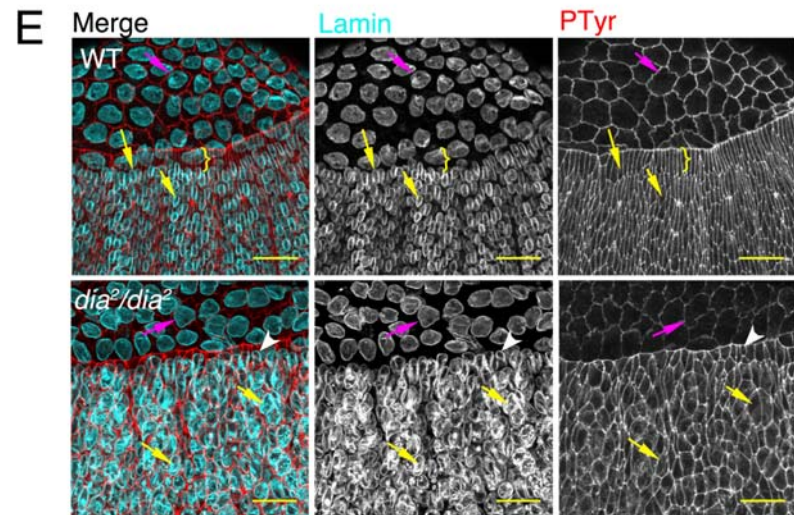
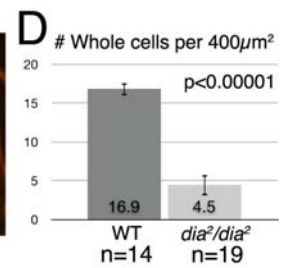
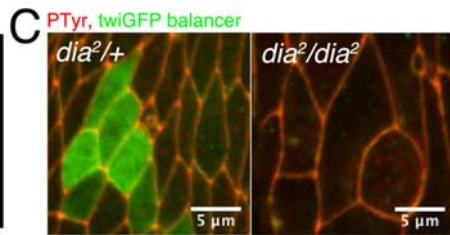
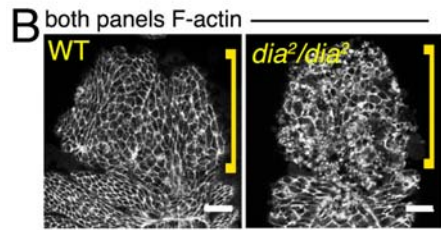
Nowotarski et al., Suppl. Figure 5

A ♀ $\frac{+}{+}$ × ♂ $\frac{+}{+}$ = 7.8% embryonic lethality (n=153) ♀ $\frac{dia^2}{+}$ × ♂ $\frac{dia^2}{+}$ = 23.8% embryonic lethality (n=483)

Cuticles of embryonic lethal *dia²/dia²* embryos



13.1% Wildtype 35.6% Anterior holes 46.0% Anterior holes with other holes: dorsal, posterior, dorsal & posterior 5.3% Severe-Scraps



Nowotarski et al.,
Suppl. Figure 6